

PACS numbers: 42.55.Rz; 42.60.Da; 42.60.Lh
DOI: 10.1070/QE2010v040n07ABEH014356

Limiting thermal regimes of active disk elements under steady-state pumping and two-dimensional temperature distribution inside the disk

A.N. Alpat'ev, D.A. Lis, V.A. Smirnov, I.A. Shcherbakov

Abstract. **An analytic expression describing the stationary two-dimensional axially symmetric temperature distribution in a disk active element (AE) is derived upon pumping the entire disk whose thickness is 0.01 cm $\leqslant h \leqslant$ 0.3 cm and the diameter-to-thickness ratio is $1 \leqslant d/h \leqslant 100$. Thermomechanical stresses are calculated. It is shown that from the point of view of the disk damage, the tangential stress on the disk side face constitutes the major threat. For different scaling parameters $x = d/h$, the limiting lasing powers P_{las} are estimated in multimode approximation, which can be obtained using a disk AE in the case of end and side cooling for different heat exchange coefficients α (by the example of an Nd:YAG crystal). It is found that the side cooling can decrease P_{las} in some situations. The priority regions are established in the space of the parameters h, x, and α which, while increasing the pump intensity, are accompanied by one of the three events violating the normal operation of the laser: deterioration of spectral and luminescent AE parameters due to heating, malfunctioning of the cooling regime, or thermomechanical damage of the disk. It is shown that an increase in the scaling parameter x smoothes the radial temperature profile and the thermoelastic stress distribution profile.**

Keywords: *disk active element, steady-state pumping, limiting lasing powers.*

1. Introduction

The problem of creating high-power disk lasers is quite urgent today [1–4]. One of the main problems in this case is the removal of a large amount of heat released in the active element (AE) because its overheating leads to deterioration of spectroscopic parameters of the working medium, formation of a thermal lens, thermoelastic stresses, and other undesirable effects.

The authors of papers [4–6] considered a one-dimensional thermal problem for a disk AE when its temperature is the function of the coordinate z (the z axis is perpendicular to the disk end faces) and is identical in any plane parallel to the end faces. This situation occurs if the pump uniform over the beam cross section illuminates the entire disk plane and the disk itself is cooled only from its end faces. In this case, one can obtain an analytic solution of the heat conduction equation and analyse different undesirable situations caused by the AE heating, which was done in [6].

In this paper, we consider a more general, two-dimensional thermal problem when the heat is removed not only through the AE end faces but also through its side face while the pump uniform over the beam cross section is absorbed due to an arbitrary number of passes and illuminates the entire AE area. As will be shown below, side cooling can lead both to an increase and a decrease in the maximal lasing power (multimode lasing) limited only by the occurrence (with increasing the pump intensity) of one of the three events undesirable for laser operation: AE heating above the prescribed temperature, malfunctioning of the normal cooling regime, thermal destruction of the AE.

2. Numerical solution of the heat conduction equation and its analytic approximation

Consider the temperature distribution of the AE in the form of disk of thickness h and radius $R = d/2$ in the case of longitudinal pumping uniform over the beam cross section (Fig. 1). The end ($z = h$) and side ($r = R$) faces of the AE are convectively cooled, the heat exchange coefficients being α_2 and α_3, respectively. In the case, when the disk is cooled by a cooling liquid indirectly, for example, though a substrate, α_2 and α_3 are the effective heat exchange coefficients taking into account the thermal resistance of the substrate. The function of the volume heat release sources q_V at any point of the disk volume is assumed identical.

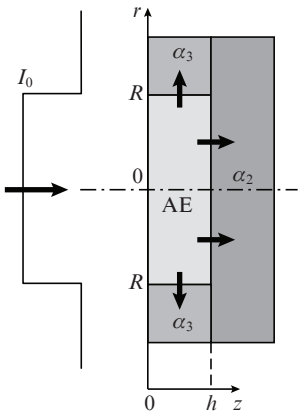

Figure 1. Two-dimensional problem: the disk AE cooling from the end face from the side $z = h$ and from the side face in the case of longitudinal uniform pumping with the intensity I_0.

A.N. Alpat'ev, D.A. Lis, V.A. Smirnov, I.A. Shcherbakov
A.M. Prokhorov Institute of General Physics, Russian Academy of Sciences, ul. Vavilova 38, 119991 Moscow, Russia;
e-mail: lisdenis@mail.ru

Received 11 May 2010
Kvantovaya Elektronika **40** (7) 604–614 (2010)
Translated by I.A. Ulitkin

This thermal problem is described by the heat conduction equation in cylindrical coordinates

$$\nabla^2 T(r,z) = -\frac{q_V}{\lambda} \tag{1}$$

with the boundary conditions of the third kind

$$\left.\frac{\partial T(r,z)}{\partial z}\right|_{z=h} = -\frac{\alpha_2}{\lambda}[T(r,h) - T_f],$$

$$\left.\frac{\partial T(r,z)}{\partial r}\right|_{r=R} = -\frac{\alpha_3}{\lambda}[T(R,z) - T_f], \tag{2}$$

the end face $z = 0$ is thermally insulated, where T_f is the temperature of the cooling media; λ is the heat conductivity.

The numerical solution of this problem shows that the temperature distribution along the z axis is close to parabolic, while the distribution over the radius r can be described by the function

$$f(\rho,m) = \frac{\cosh m - \cosh(\rho m)}{\cosh m - 1}, \tag{3}$$

where $\rho = r/R$;

$$m = C\frac{2R}{h}\sqrt{\frac{\alpha_2 h}{2\lambda}}; \tag{4}$$

C is the dimensionless quantity.

The behaviour of the function $f(\rho,m)$ as a function of ρ for several values of m is shown in Fig. 2. With decreasing m, the function $f(\rho,m)$ gives a parabolic temperature distribution, while with increasing m – a temperature distribution of 'shelf' type:

$$f(\rho,m) = \begin{cases} 1-\rho^2, & m \to 0, \\ 1, & m \to \infty. \end{cases}$$

Therefore, it is logical to call m the smoothing parameter and $f(\rho,m)$ – the smoothing function.

The approximate analytic solution of equation (1) with boundary conditions (2) has the form

$$T(\rho,z) = \Delta T_1(0,0)\left[f(\rho,m) + \frac{1}{M}\right]H(z) + T_f, \tag{5}$$

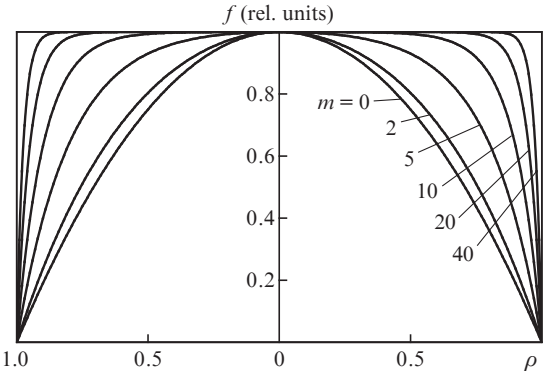

Figure 2. Smoothing function $f(\rho,m)$.

where

$$\Delta T_1(0,0) = T(0,0) - T(R,0) = q_V\frac{RKM}{2\alpha_3\Psi};$$

$$H(z) = \left(1 - \frac{z^2}{h^2}\right)\frac{K-1}{K} + \frac{1}{K};$$

$$\Psi = K + \frac{R}{2h}\frac{\alpha_2}{\alpha_3} + \frac{\alpha_2}{2\lambda}\frac{R^2}{h}F(m);$$

$$F(m) = \frac{1}{m}\left[\frac{1}{\tanh m} - \frac{2}{m} + \frac{2}{m^2}\tanh\left(\frac{m}{2}\right)\right];$$

the constants $M = (\alpha_3 R/\lambda)\tanh(m/2)/m$ and $K = 1 + \alpha_2 h/(2\lambda)$ are obtained from boundary conditions (2) on the side and end surfaces, respectively. Let us introduce also the following notations (Fig. 3):

$$\Delta T_1(0,h) = T(0,h) - T(R,h),$$

$$\Delta T_2(R,0) = T(R,0) - T_f,\ \ \Delta T_2(R,h) = T(R,h) - T_f,$$

$$\Delta T_1(0,z) = T(0,z) - T(R,z),\ \ \Delta T_2(R,z) = T(R,z) - T_f,$$

$$\Delta T(0,0) = T(0,0) - T_f = \Delta T_1(0,0) + \Delta T_2(R,0),$$

$$\Delta T(0,h) = T(0,h) - T_f = \Delta T_1(0,h) + \Delta T_2(R,h),$$

$$\Delta T(0,z) = T(0,z) - T_f = \Delta T_1(0,z) + \Delta T_2(R,z),$$

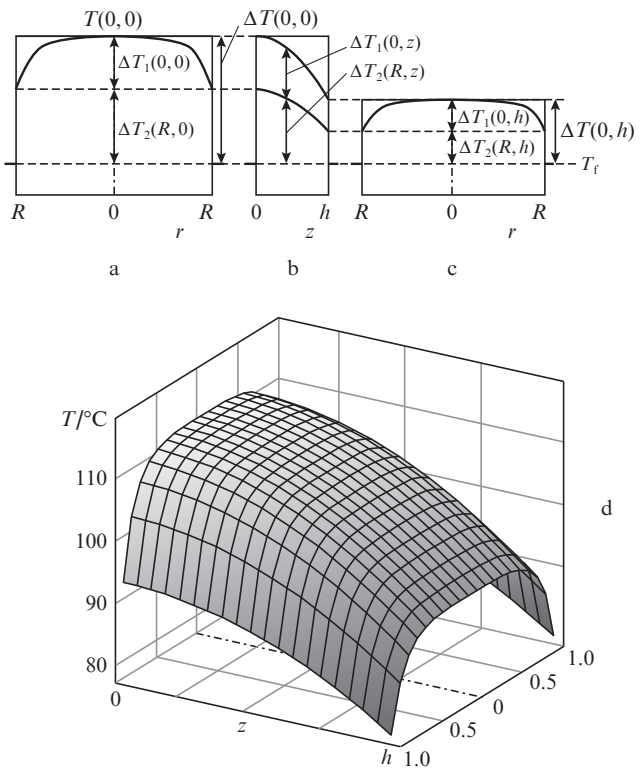

Figure 3. Characteristic temperature distribution in the disk with respect to the cuts $z = 0$ (a), $r = 0 - R$ (b), and $z = h$ (c) as well as the three-dimensional temperature profile plotted at $d = 2$ cm, $h = 0.1$ cm, $q_V = 500$ W cm^{-3}, $\alpha_2 = 0.75$ W cm^{-2} K^{-1}, $\alpha_3 = 0.25$ W cm^{-2} K^{-1}, $T_f = 27$ °C (d).

where the subscript 1 corresponds to the internal temperature drop (between the axis and the side face) and the subscript 2 – to the external temperature drop (between the temperature of the side face and the temperature T_f), the temperature drops without subscripts – are the general drops (between the temperature on the axis and T_f). The relation between the introduced parameters has the form:

$$\Delta T_1(0,0) = K\Delta T_1(0,h), \tag{6}$$

$$\Delta T_2(R,0) = K\Delta T_2(R,h), \tag{7}$$

$$\Delta T_1(0,0) = M\Delta T_2(R,0), \tag{8}$$

$$\Delta T_1(0,h) = M\Delta T_2(R,h). \tag{9}$$

The obtained analytic expression (5) for $T(r,z)$, with the accuracy no worse than ~10% (with respect to the numerical solution) at $\lambda = 0.13$ W cm^{-1} K^{-1} (YAG crystal) and the values of α_2 and α_3 used in calculations, describes the temperature distribution in the disk at least in the range under study $d/h = 1$–100 (where $h = 0.01$–0.3 cm) for $C = 0.62$. For thicknesses $h > 0.3$ cm, the value of the parameter C should be specified; for example, for $h = 0.5$ cm, we have the constant $C \approx 0.5$.

If the end or side faces of the disk are heat insulated, then, setting $\alpha_2 = 0$ or $\alpha_3 = 0$, respectively, in expression (5), we obtain known one-dimensional temperature distributions under steady-state pumping:

$$T(r) = \frac{q_V}{4\lambda}(R^2 - r^2) + \frac{q_V R}{2\alpha_3} + T_f \tag{10a}$$

for a cylinder unlimited in z (which is equivalent to $\alpha_2 = 0$ for a cylinder of an arbitrary size) and

$$T(z) = \frac{q_V}{2\lambda}(h^2 - z^2) + \frac{q_V h}{\alpha_2} + T_f \tag{10b}$$

for a disk with an unlimited end face (which is equivalent to $\alpha_3 = 0$ for a disk of an arbitrary size). Note that all this allows one to extrapolate the analytic expression for the temperature distribution (5) to the regions $d/h < 1$ and $d/h > 100$.

Expression (5) yields also particular solutions with the boundary conditions of the first kind on the end and side faces at $\alpha_2 = \infty$ and $\alpha_3 = \infty$, respectively.

For a convenience of the analysis of thermal processes proceeding during scaling (i.e., when changing the ratio between the disk diameter d and thickness h), we will introduce the scaling parameter $x = d/h$. Then,

$$\Delta T_1(0,0) = q_V \frac{xhKM}{4\alpha_3 \Psi(x)},$$

where

$$\Psi(x) = K + x\frac{\alpha_2}{4\alpha_3} + x^2\frac{\alpha_2 h}{8\lambda}F(m);$$

$$M = \frac{\alpha_3 hx}{2\lambda}\frac{\tanh(m/2)}{m}; \quad m = xC\sqrt{\frac{\alpha_2 h}{2\lambda}}.$$

Let us estimate the applicability of the constant function of thermal sources q_V. To this end, we will use the real function $q_V(z)$ obtained in [6]:

$$q_V(z) = \xi I_0 \eta_{abs} k \frac{\cosh[k(z-h)]}{\sinh(kh)}, \tag{11}$$

where ξ is the fraction of the absorbed pump power transformed to heat; $\eta_{abs} = 1 - \exp(-nkh)$ is the fraction of the pump power absorbed in the crystal after n passes; k is the pump absorption coefficient constant over the entire AE volume (which is possible, for example, when the pump intensity exceeds the threshold).

We obtain from (11) an average integral function of the heat release sources

$$\bar{q}_V = \frac{1}{h}\int_0^h q_V(z)\mathrm{d}z = \xi I_0 \frac{\eta_{abs}}{h}.$$

Then, the pump intensity has the form

$$I_0 = \frac{\bar{q}_V h}{\xi \eta_{abs}}. \tag{12}$$

The ratio of the different $\Delta q_V = q_V(0) - q_V(h)$ of real heat release function (11) at points $z = 0$ and $z = h$ to the average integral function $\bar{q}_V$ has the form

$$\frac{\Delta q_V}{\bar{q}_V} = D\frac{\cosh D - 1}{\sinh D},$$

where $D = kh$ is the optical density. This ratio changes by no more than ~1% at $D \sim 0.14$ and by no more than ~10% at $D \sim 0.45$. Therefore, after selecting the disk thickness, we can find k. For example, for the approximation $q_V = \text{const}$ with an accuracy up to ~10% at $h = 0.01$ and 0.1 cm, $k \leqslant 45$ cm^{-1} and $k \leqslant 4.5$ cm^{-1}, respectively, are required.

3. Critical function of thermal sources and the pump intensity during scaling

At the temperature of water starting boiling (we will call it the critical event B), which cools the disk end face from the side $z = h$ (Fig. 4), we can obtain from (5) an expression for the function of heat release sources and from (12) – for the input

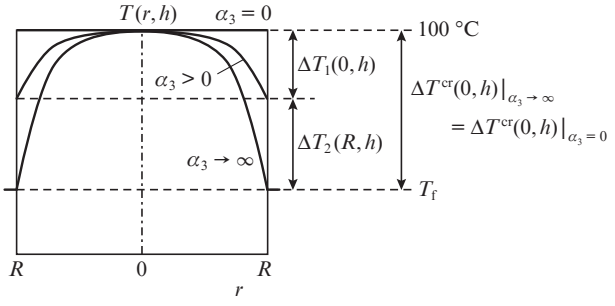

Figure 4. Characteristic critical temperature distributions on the end face $z = h$ for a disk with a heat-insulated side face ($\alpha_3 = 0$), a disk with a real heat conducting side face ($\alpha_3 > 0$, boundary conditions of the third kind), and a disk with a side face ideally conducting heat ($\alpha_3 \to \infty$, boundary conditions of the first kind).

pump intensity. From the expression for the temperature drop (at $r = 0$ and $z = h$)

$$\Delta T^{\rm cr}(0,h) + T_{\rm f} = T^{\rm cr}(0,h) = q_V^{\rm B}\frac{xh(M+1)}{4\alpha_3\Psi(x)} + T_{\rm f} = 100\,^{\circ}{\rm C},$$

we obtain the critical function of thermal sources

$$q_V^{\rm B} = \Delta T^{\rm cr}(0,h)\frac{4\alpha_3\Psi(x)}{xh(M+1)}. \qquad (13)$$

For the one-dimensional case (10) ($\alpha_3 = 0$ or $x \to \infty$), we have

$$\Delta T^{\rm cr}(0,h)\big|_{\alpha_3=0} + T_{\rm f} = q_V^{\rm B}\big|_{\alpha_3=0}\frac{h}{\alpha_2} + T_{\rm f} = 100\,^{\circ}{\rm C}.$$

It follows from here that

$$q_V^{\rm B}\big|_{\alpha_3=0} = \Delta T^{\rm cr}(0,h)\frac{\alpha_2}{h}. \qquad (14)$$

Figure 5 shows the dependence of the critical pump intensity (for the event B) on k for $\alpha_2 = 0.75$ W cm^{-2} K^{-1} and the number of pump passes $n = 2$ and 16.

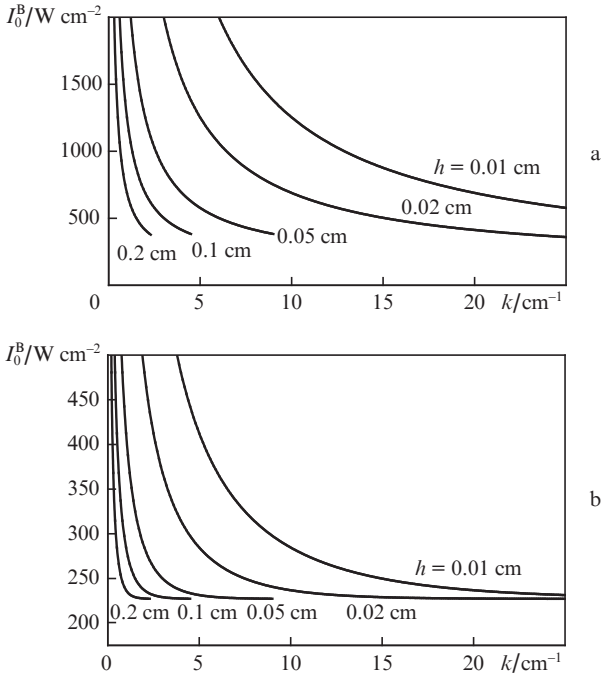

Figure 5. Critical pump intensity leading to water boiling on the end face $z = h$ at $\alpha_3 = 0$, $\alpha_2 = 0.75$ W cm^{-2} K^{-1} and different disk thicknesses as a function of the pump absorption coefficient. The number of pump passes $n = 2$ (a) and 16 (b).

In the case of boundary conditions of the first kind ($\alpha_3 \to \infty$) on the side face, we obtain from the expression for the temperature drop (at $r = 0$ and $z = h$)

$$\Delta T^{\rm cr}(0,h) = 100\,^{\circ}{\rm C} - T_{\rm f} = q_V^{\rm B}\big|_{\alpha_3\to\infty}\frac{x^2h^2\tanh(m/2)}{8\lambda m\Psi(x)\big|_{\alpha_3\to\infty}},$$

where

$$\Psi(x)\big|_{\alpha_3\to\infty} = K + x^2\frac{\alpha_2 h}{8\lambda}F(m);$$

$$q_V^{\rm B}\big|_{\alpha_3\to\infty} = \Delta T^{\rm cr}(0,h)\frac{8\lambda m\Psi(x)\big|_{\alpha_3\to\infty}}{x^2h^2\tanh(m/2)}. \qquad (15)$$

When the temperature of water starting boiling on the disk end face $z = h$ is achieved, the temperature $T(0,0)$ at point $r = 0$, $z = 0$ can be found with the help of expressions (6) and (7). Because this temperature is the maximal disk temperature, its value should not exceed some threshold whose excess noticeably impairs the spectral and luminescent properties of active ions (the event D), which should be taken into account in calculations of thermal regimes. In this case,

$$\Delta T^{\rm D}(0,0) = K\Delta T^{\rm cr}(0,h), \qquad (16)$$

where $\Delta T^{\rm D}(0,0) = \Delta T_1(0,0) + \Delta T_2(R,0)$; $\Delta T^{\rm cr}(0,h) = \Delta T_1(0,h) + \Delta T_2(R,h)$.

4. Thermoelastic stresses in the disc during scaling. Limiting function of thermal sources and the pump intensities corresponding to the disk damage (event C)

4.1. Thermoelastic stresses

Tangential σ_φ (perpendicular to the radius r and the axis z) and radial σ_r stresses for the axially symmetric temperature distribution $T(r,z)$ are determined, according to [7], by the expressions

$$\sigma_\varphi = \frac{N_\varphi}{h} + \frac{12}{h^3}M_\varphi\left(z - \frac{h}{2}\right) + \frac{E}{1-\nu}\left[\varepsilon_T + \chi_T\left(z - \frac{h}{2}\right) - \alpha_T\Delta T\right], \qquad (17)$$

$$\sigma_r = \frac{N_r}{h} + \frac{12}{h^3}M_r\left(z - \frac{h}{2}\right) + \frac{E}{1-\nu}\left[\varepsilon_T + \chi_T\left(z - \frac{h}{2}\right) - \alpha_T\Delta T\right], \qquad (18)$$

where N_φ, N_r and M_φ, M_r are the internal thermal stress and moment resultants; ε_T and χ_T are the generalised thermal expansion and bending, respectively; α_T is the average coefficient of linear thermal expansion of the disk material; E and ν are the elasticity modulus (Young modulus) and the Poisson coefficient, respectively.

We will not consider the longitudinal component of the stresses σ_z because the thin disk is characterised by a plane stress state at which $\sigma_z \approx 0$ [8].

Substituting the expression

$$\Delta T(\rho,z) = T(\rho,z) - \Delta T_2(R,h) - T_{\rm f} = \Delta T_1(0,0)\left[f(\rho,m) + \frac{1}{M}\right]H(z) - \frac{\Delta T_1(0,0)}{KM}$$

into (17) and (18) and using the boundary conditions for a thin disk free of external stresses, when $N_r = 0$, $N_\varphi = 0$, $M_r = 0$, $M_\varphi = 0$ on its side face, we derive expressions (17) and (18) in the form

$$\sigma_\varphi(\rho,z) = \gamma\Delta T_1(0,0)$$

$$\times\left\{L(\rho)D(z)(1-\nu)+\left[f(\rho,m)+\frac{1}{M}\right][D(z)-H(z)]\right\}, \quad (19)$$

$$\sigma_r(\rho,z) = \gamma\Delta T_1(0,0)$$

$$\times\left\{P(\rho)D(z)(1-\nu)+\left[f(\rho,m)+\frac{1}{M}\right][D(z)-H(z)]\right\}, \quad (20)$$

where $\gamma = E\alpha_T/(1-\nu)$;

$$D(z) = \frac{1}{h}\int_0^h H(z)\mathrm{d}z + \left(z-\frac{h}{2}\right)\frac{12}{h^2}\int_0^h H(z)\left(z-\frac{h}{2}\right)\mathrm{d}z$$

$$= \frac{2K+1}{3K} + \frac{1-K}{hK}\left(z-\frac{h}{2}\right),$$

$$L(\rho) = \int_0^1 \rho f(\rho,m)\mathrm{d}\rho - f(\rho,m) + \frac{1}{\rho^2}\int_0^\rho \rho f(\rho,m)\mathrm{d}\rho$$

$$= \frac{m}{2\tanh(m/2)}\left[F(m)+\frac{F(\rho,m)}{\rho^2}\right] - f(\rho,m);$$

$$P(\rho) = \int_0^1 \rho f(\rho,m)\mathrm{d}\rho - \frac{1}{\rho^2}\int_0^\rho \rho f(\rho,m)\mathrm{d}\rho$$

$$= \frac{m}{2\tanh(m/2)}\left[F(m)-\frac{F(\rho,m)}{\rho^2}\right];$$

$$F(\rho,m) = \frac{1}{m}\left\{\frac{\rho^2}{\tanh m} - \frac{2}{m}\frac{\rho\sinh(\rho m)}{\sinh m}\right.$$

$$\left.+\frac{2}{m^2}\left[\frac{\cosh(\rho m)-1}{\cosh m-1}\right]\tanh\left(\frac{m}{2}\right)\right\}.$$

Note that at $\alpha_2 \to 0$ with an accuracy to the cofactor $(1-\nu)$, expressions (19) and (20) describe stresses in a cylinder:

$$\sigma_\varphi(\rho) = \gamma q_V\frac{R^2}{16\lambda}(3\rho^2-1)(1-\nu),$$

$$\sigma_r(\rho) = \gamma q_V\frac{R^2}{16\lambda}(\rho^2-1)(1-\nu),$$

and at $\alpha_3 \to 0$ – the stresses in the plate (see, for example, [7–9]):

$$\sigma_\varphi(z) = \sigma_r(z) = \gamma q_V\frac{hK}{\alpha_2}[D(z)-H(z)].$$

Figure 6 shows the radial distribution of stresses σ_φ and σ_r in the YAG disk of thickness $h = 0.1$ cm at $z = 0$, $q_V = 500$ W cm^{-3}, $\alpha_2 = \alpha_3 = 0.75$ W cm^{-2} K^{-1}, $x = 1$–100. One can see that when changing the scaling parameter x, the sign of the stress on the disk axis changes from positive (at $x = 1$–1.71) to negative (at $x = 1.71$–25.6) and vice versa (at $x > 25.6$). The maximal negative values of σ_φ and σ_r on the axis are achieved at $x = 4.7$. Note that an increase in x and thus in m smoothes not only the temperature profile in the disk but also the stress profile. Interestingly, the stresses σ_φ, σ_r were calculated above assuming that expressions (17) and (18) obtained in [7] for a thin disk give a correct estimate of the stresses up to $x = 1$.

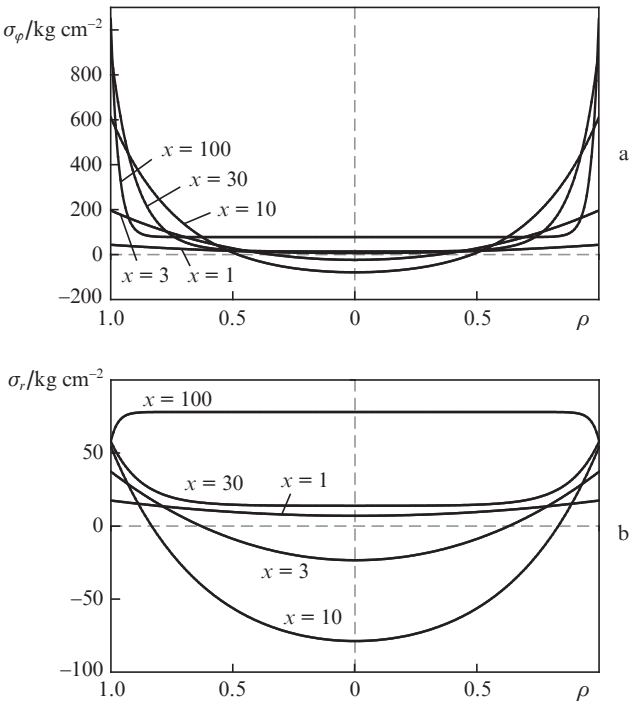

Figure 6. Distributions of tangential (a) and radial (b) stresses over the radius at $z = h$ in the disk of thickness $h = 0.1$ cm at $q_V = 500$ W cm^{-3}, the heat exchange coefficients $\alpha_2 = \alpha_3 = 0.75$ W cm^{-2} K^{-1} and different scaling parameters x.

Let us present the expressions for the stresses on the input end face ($z = 0$) on the axis and the side face of the disk surface. Because at $z = 0$ we have $D = (7K-1)/(6K)$, $D - H = (K-1)/(6K)$, at $\rho = 1$, $L = mF(m)/\tanh(m/2)$, $P = 0$ and at $\rho = 0$, $L = P = {}^1/_2[mF(m)/\tanh(m/2) - 1]$, by substituting these expressions into (19) and (20) we obtain

$$\sigma_r(0,0) = \gamma\Delta T_1(0,0)\left\{\frac{1}{2}\left[\frac{mF(m)}{\tanh(m/2)}-1\right]\right.$$

$$\left.\times\frac{7K-1}{6K}(1-\nu)+\left(1+\frac{1}{M}\right)\frac{K-1}{6K}\right\},$$

$$\sigma_r(1,0) = \gamma\Delta T_1(0,0)\frac{1}{M}\frac{K-1}{6K} \quad (21a)$$

for the radial stress at the centre and on the side, respectively, and

$$\sigma_\varphi(0,0) = \sigma_r(0,0),$$
$$\sigma_\varphi(1,0) = \gamma\Delta T_1(0,0) \times\left[\frac{mF(m)}{\tanh(m/2)}\frac{7K-1}{6K}(1-\nu)+\frac{1}{M}\frac{K-1}{6K}\right] \quad (21б)$$

for the tangential stress at the centre and on the side.

4.2. Maximal temperature drop $\Delta T_1^{\mathrm{C}}(0,0)$ at the moment of thermal damage

Of all the stresses, the greatest is the tangential (hoop) tensile stress on the side (21) at $z = 0$, $\rho = 1$ with some temperature drop $\Delta T_1^{\mathrm{C}}(0,0)$ corresponding to it. When the stress σ_{s} reaches the maximal value corresponding to the disk damage, the temperature drop will be determined by the expression

$$\Delta T_1^{\mathrm{C}}(0,0) = \frac{\sigma_{\mathrm{s}}}{\gamma}\frac{1}{\Theta(x)}, \quad (22)$$

where

$$\Theta(x) = \frac{1}{6KM}\left[\frac{\alpha_3 h}{2\lambda}xF(m)(7K-1)(1-\nu)+K-1\right].$$

In the limiting cases $x \to 0$ and $x \to \infty$ and taking into account that fact that the smoothing degree m is proportional to the scaling parameter x (at constant h), we obtain

$$\Delta T_1^{\mathrm{C}}(0,0) = \frac{\sigma_{\mathrm{s}}}{\gamma}\begin{cases}0, & x\to 0, m\to 0,\\ \dfrac{6K}{(7K-1)(1-\nu)+(\mathrm{C}\alpha_2/\alpha_3)\sqrt{\alpha_2 h/(2\lambda)}}, & x\to\infty, m\to\infty.\end{cases}$$

Figure 7 presents the temperature drop $\Delta T_1^{\mathrm{C}}(0,0)$ at $z = 0$ at the moment of the damage of the 0.1-cm-thick disk as a function of the scaling parameter x for $\alpha_2 = \alpha_3 = 0.75$ W cm^{-2} K^{-1} ($\sigma_{\mathrm{s}} = 2008$ kg cm^{-2}, $\gamma = 34$ kg cm^{-2} deg^{-1}, $\nu = 0.25$). At $x = 4.7$ ($m = 1.54$) the temperature drop has a strongly pronounced maximum 123 °C, and at $x > 40$ ($m > 10$) the temperature drop asymptotically tends to 72 °C. When the disk thickness is increased, the amplitude of the maximum decreases and the maximum is displaced towards smaller x: for example, at $h = 0.3$ cm, $x = 2.9$ ($m = 1.67$) the maximal temperature drop is 116 °C, and at $x > 20$ the drop $\Delta T_1^{\mathrm{C}}(0,0) \to 69$ °C. When the disk thickness is decreased, the amplitude of the maximum increases and the maximum is displaced towards larger x: for example, at $h = 0.01$ cm, $x = 11$ ($m = 1.17$) the maximal temperature drop is 140 °C, and at $x > 100$ the drop $\Delta T_1^{\mathrm{C}}(0,0) \to 77$ °C.

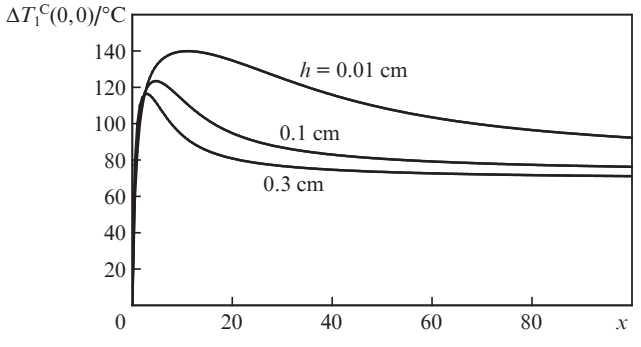

Figure 7. Maximal temperature drop $\Delta T_1^{\mathrm{C}}(0,0)$ at the moment of thermal destruction as a function of the scaling parameter at different disk thicknesses h.

4.3. Limiting function of thermal sources

Substituting the expression for the maximal temperature drop (22) into (5), we obtain the expression for the limiting function of thermal sources, corresponding to the disk damage:

$$q_V^{\mathrm{C}} = \frac{\sigma_{\mathrm{s}}}{\gamma}\frac{4\alpha_3\Psi(x)}{xhKM(x)}\frac{1}{\Theta(x)}, \quad (23)$$

and using expression (12), we find the input pump intensity.

In the case of boundary conditions of the first kind ($\alpha_3 \to \infty$) on the side face, the limiting function of thermal sources, corresponding to the disk damage, has the form

$$q_V^{\mathrm{C}}\big|_{\alpha_3\to\infty} = \frac{\sigma_s}{\gamma}\frac{8\lambda\Psi(x)\big|_{\alpha_3\to\infty}}{x^2h^2}\frac{6}{F(m)(7K-1)(1-\nu)}. \quad (24)$$

Obviously, in the one-dimensional problem (10), at $\alpha_3 = 0$ the limiting function of thermal sources corresponding to the plate damage has the form

$$q_V^{\mathrm{C}}\big|_{\alpha_3=0} = \frac{\sigma_s}{\gamma}\frac{12\lambda}{h^2}. \quad (25)$$

5. Calculation of the priority zones of the event occurrence – boiling (B), damage (C), or achievement of the prescribed maximum disk temperature (D)

It follows from (16) that when the pump is uniform, the temperature drop along the disk axis depends only on K and is independent of x (for all the above-considered boundary conditions on the side face). Therefore, at the disk thickness smaller than that determined by the expression

$$h^{\mathrm{D}} = \frac{2\lambda}{\alpha_2}\left[\frac{\Delta T^{\mathrm{D}}(0,0)}{\Delta T^{\mathrm{cr}}(0,h)}-1\right], \quad (26)$$

(with increasing the pump intensity) the critical temperature of the rear end face (for example, corresponding to the start of water boiling) is first achieved. And vice verse, if the disk thickness is larger than h^{D}, first, the temperature $T^{\mathrm{D}}(0,0)$ achieves the specified value and then, the critical temperature of the rear end face $T^{\mathrm{cr}}(0,h)$ is achieved.

As a maximally possible temperature whose excess significantly affects the spectral and luminescent properties of the AE, we chose the temperature 200 °C (the temperature below 200 °C is usually considered acceptable for the Nd:YAG crystal). The estimates show that at the disk thicknesses $h \leqslant 0.3$ cm used in this paper, the event B (start of the water boiling) occurs (with increasing the pump intensity) prior to the event D (achievement of the temperature 200 °C at the 'hottest' point of the disk $r = 0$, $z = 0$); therefore, we consider below only the events B and C (thermomechanical damage of the disk).

Equating expressions (13) and (23) to each other, we obtain the interface separating the priority zones of the event occurrence – water boiling (B) or disk damage (C) – with increasing the pump intensity in the space of the parameters h and x (Fig. 8). In this case, h and x are related by the expression

$$\frac{\Delta T^{\mathrm{cr}}(0,h)\gamma}{\sigma_{\mathrm{s}}} = \frac{M(x)+1}{KM(x)\Theta(x)}. \tag{27}$$

Note that this expression is independent of the heat release fraction ξ and the number of passes of the pump n in the disk. As a result, the boundary of the regions B and C will correspond to different pump regimes, for example, lamp (broadband) and diode (selective) pumping.

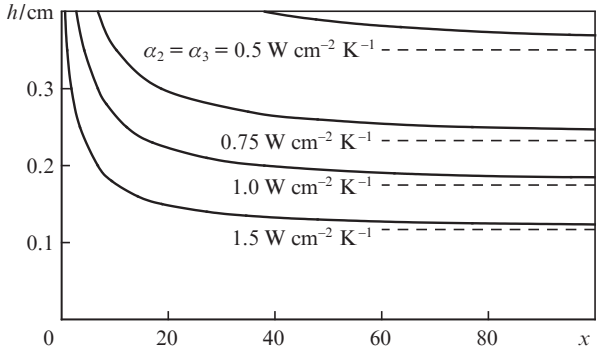

Figure 8. Calculated disk thicknesses determining the boundary of priority zones of the event occurrence (start of water boiling and disk damage) versus the scaling parameter x with increasing the pump power for different heat exchange coefficients $\alpha_2 = \alpha_3$. The area above the curves is thermal damage of the disk; below – start of water boiling. Dashed curves are the asymptotic values of the disk thickness.

In the particular case $x \to \infty$, expression (27) allows one to find the optimal disk thickness such that the start of the coolant boiling is only possible at h smaller than the determined thickness. To this end, expression (27) can be rewritten in the form (for the YAG crystal)

$$\frac{\alpha_2}{\alpha_3} \approx 6\frac{\sqrt{\mathrm{Bi}}(\mathrm{Bi}-0.14)}{9.72-\mathrm{Bi}},$$

where $\mathrm{Bi} = \alpha_2 h/\lambda$ is the Biot number (the ratio of the internal thermal resistance of the AE to the external thermal resistance of its end face during the thermal flow along the z axis). For example, at the interface between the zones B and C (Fig. 8), when $x \to \infty$, $\alpha_2 = \alpha_3 = 0.5$, 0.75, 1.0, and 1.5 W cm^{-2} K^{-1}, the thicknesses asymptotically tend to minimal values 0.35, 0.233, 0.175, and 0.117 cm, respectively, which are found from the expression $h = \mathrm{Bi}\lambda/\alpha_2$, where Bi = 1.346. The ratio α_2/α_3 can be approximated by the expression $\alpha_2/\alpha_3 \approx \mathrm{Bi}^2/2$ (with an accuracy $\sim 10\%$) at $0 \leqslant \mathrm{Bi} \leqslant 4.4$.

6. Maximal lasing power of a disk four-level laser limited by one of the critical evens as a function of the scaling parameter

Based on the found critical (B) and limiting (C) pump powers and the priority zones established for them in the space of the parameters h and x, we can estimate the maximal lasing power of a disk laser with one AE in the resonator (multimode approximation).

The four-level lasing intensity under steady-state pumping is described, as is known, by the expression

$$I_{\mathrm{las}} = \frac{a}{a+2\chi h}\frac{\hbar\omega_{\mathrm{las}}}{\hbar\omega_{\mathrm{pump}}}\eta_{\mathrm{abs}}(I_0 - I_{\mathrm{th}}), \tag{28}$$

where $a = \ln R_{\mathrm{out}}^{-1}$; R_{out} is the reflectivity of the output resonator mirror at the laser wavelength (the rear resonator mirror is highly reflecting); χ is the coefficient of passive losses in the resonator; $\hbar\omega_{\mathrm{las}}$ и $\hbar\omega_{\mathrm{pump}}$ are the energies of laser and pump quanta, respectively; η_{abs} is the fraction of the absorbed pump power; I_0, I_{th} are the input and threshold pump intensities, respectively.

It is obvious that the quantities η_{abs} and I_{th} are subjected to the temperature effects due to a change in the spectroscopic properties of the AE during the heating (because of the Boltzmann population of the Stark levels, temperature pump absorption line broadening and the temperature luminescence line broadening of the working laser level, etc.). When the AE temperature is increased, η_{abs} decreases, while I_{th} increases, which affects the laser efficiency.

For each AE thickness h, expression (28) allows one to find the maximal lasing intensity for the corresponding optimal reflectivity of the output mirror (i.e., for the optimal a_{opt}), which is determined from the expression $\partial I_{\mathrm{las}}/\partial a = 0$ with the substitution of the pump intensity by the function of thermal sources according to expression (12), where $\bar{q}_V \simeq q_V$, with an accuracy $\sim 10\%$. Then the maximal lasing intensity for a 1.064-μm Nd:YAG laser is

$$I_{\mathrm{las}}^{\max} = \frac{a_{\mathrm{opt}}}{a_{\mathrm{opt}}+2\chi h}\frac{\hbar\omega_{\mathrm{las}}}{\hbar\omega_{\mathrm{pump}}}\frac{q_V h}{\xi} - \frac{a_{\mathrm{opt}}\hbar\omega_{\mathrm{las}}}{2\sigma_{\mathrm{las}}\tau}, \tag{29}$$

where $a_{\mathrm{opt}} = C_1 h\sqrt{q_V} - 2\chi h$; $C_1 = 2\sqrt{\chi\sigma_{\mathrm{las}}\tau/(\hbar\omega_{\mathrm{pump}}\xi)}$; $\sigma_{\mathrm{las}} = 2.85\times10^{-19}$ cm^2 is the effective laser cross section; $\tau = 250$ μs is the lifetime of the working laser level.

In deriving (29) we used the threshold condition for which the pump absorption coefficient ($\lambda_{\mathrm{pump}} = 0.808$ μm) $k = \sigma_{\mathrm{pump}}[N_0 - (a+2\chi h)/(2\sigma_{\mathrm{las}}h)]$, where $\sigma_{\mathrm{pump}} = 1.5\times10^{-19}$ cm^2 is the effective pump absorption cross section, and assumed that the entire population of the active Nd^{3+} ion with the concentration $N_0 = 6.9\times10^{19}$ cm^{-3} (0.5 at.%) is distributed only between the ground state and the working laser level of the Nd^{3+} ion ($\chi = 0.005$ cm^{-1}).

Depending on the event to be considered – B ($q_V = q_V^{\mathrm{B}}$) or C ($q_V = q_V^{\mathrm{C}}$), we will use in expression (29) the notations $I_{\mathrm{las}}^{\mathrm{B}}$ or $I_{\mathrm{las}}^{\mathrm{C}}$, respectively, for the maximal lasing intensity. The expressions for the maximal lasing power, limited by one of the events – B or C, have the form

$$P_{\mathrm{las}}^{\mathrm{B}} = I_{\mathrm{las}}^{\mathrm{B}} S, \tag{30}$$

$$P_{\mathrm{las}}^{\mathrm{C}} = I_{\mathrm{las}}^{\mathrm{C}} S, \tag{31}$$

where $S = \pi R^2 = \pi x^2 h^2/4$ is the area of the AE end surface.

When the value of α_2 is specified, in the particular case of the heat-insulated side surface ($\alpha_3 = 0$), for $h \to 0$ we obtain from (29) at $q_V = q_V^{\mathrm{B}}\big|_{\alpha_3=0}$ (14)

$$P_{\mathrm{las}}^{\mathrm{B}} \to \frac{\hbar\omega_{\mathrm{las}}}{\hbar\omega_{\mathrm{pump}}}\frac{\Delta T^{\mathrm{cr}}(0,h)\alpha_2}{\xi}S. \tag{32}$$

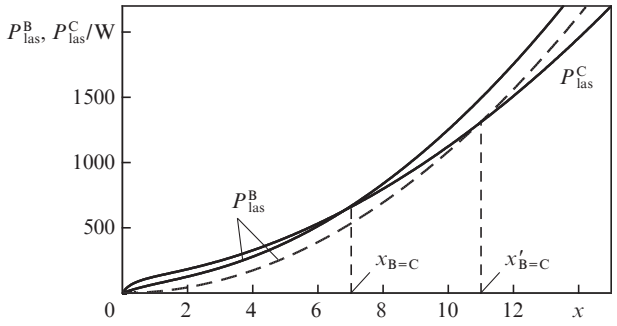

Figure 9. Calculated maximal lasing powers limited by the event B or C as functions of the scaling parameter x at $h = 0.2$ cm, $\alpha_2 = \alpha_3 = 1.5$ W cm^{-2} K^{-1} (solid curves) and $\alpha_2 = 1.5$ W cm^{-2} K^{-1} and $\alpha_3 = 0$ (dashed curves).

Figure 9 presents the lasing powers obtained from expressions (30) and (31) at $h = 0.2$ cm and $\alpha_2 = \alpha_3 = 1.5$ W cm^{-2} K^{-1} as well as in the case of the heat-insulated side face at $\alpha_2 = 1.5$ W cm^{-2} K^{-1} and $\alpha_3 = 0$.

Note that at $\alpha_3 \to \infty$ or $\alpha_3 \to 0$ and with a simultaneous increase in x, expressions (30) asymptotically converge to parabolic dependences of x, while expressions (31) diverge, in the case of large x the power P^{C}_{las} at $\alpha_3 \to 0$ being greater than that at $\alpha_3 \to \infty$. However, there exists the heat exchange coefficient $\alpha_3^{B=C} = 0.59$ W cm^{-2} K^{-1}, at which expressions (30) and (31), with increasing x, asymptotically converge to one and the same parabolic dependence, similar to expression (30) at $\alpha_3 \to 0$, i.e., $P^{C}_{las} = P^{B}_{las}\big|_{\alpha_3 \to 0} \simeq P^{B}_{las}\big|_{\alpha_3 \to \infty}$ at $x \to \infty$.

At other α_2 and h, the quantity $\alpha_3^{B=C}$ for which at large x the events B and C occur simultaneously, is shown in Fig. 10. At $\alpha_3 \leqslant \alpha_3^{B=C}$, the maximum power P_{las} is limited only by the start of water boiling, and at $\alpha_3 > \alpha_3^{B=C}$ the disk is damaged and the quantity $x_{B=C}$ separating these two events is found from expressions (30) and (31).

For small powers (less than 5–50 W at $x \to 0$), expressions (30) and (31), depending on α_3, have the form

$$P^{B}_{las} = A\Delta T^{cr}(0,h)\begin{cases} hK, & \alpha_3 \to \infty,\ x \to 0, \\ 0, & \alpha_3 \to 0,\ x \to 0, \end{cases} \tag{33}$$

$$P^{C}_{las} = A\frac{\sigma_s}{\gamma}\begin{cases} \dfrac{12hK}{(7K-1)(1-\nu)}, & \alpha_3 \to \infty,\ x \to 0, \\ 0, & \alpha_3 \to 0,\ x \to 0, \end{cases} \tag{34}$$

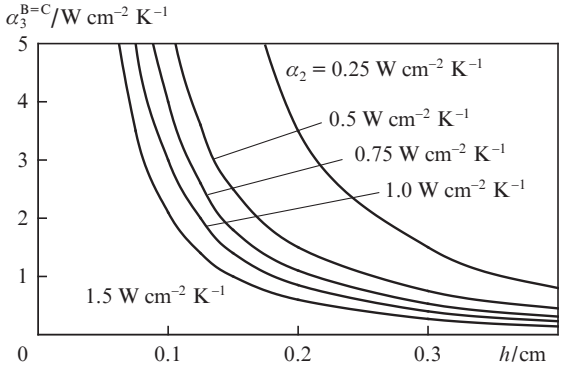

Figure 10. Calculated heat exchange coefficient $\alpha_3^{B=C}$ on the side face being cooled as a function of the disk thickness at different α_2.

where

$$A = \frac{\hbar\omega_{las}}{\hbar\omega_{pump}}\frac{4\pi\lambda}{\xi}.$$

To obtain the real value of P^{C}_{las} in expression (34), the cofactor $(1 - \nu)$ should be replaced by 1. With 1 in place of $(1 - \nu)$ for Θ in (22), the maximum lasing power limited by one of the events – B or C, can be found from expressions (30) and (31) as well as at the scaling parameter $x < 1$ (i.e., for a cylindrical AE at $h < 0.3$ cm). Note that at $x < 1$, the stress σ_z should be taken into account; nevertheless, the maximal stress corresponding to the AE damage is the tensile stress $\sigma_\varphi(1,0)$ (21) on the side face of the AE surface.

Consider the influence of the end (determined by the heat exchange coefficient α_2) and side (α_3) cooling of the disk on the increase in the lasing power P_{las}. The effect of side cooling is not so unambiguous as that of the end cooling.

The analysis of the characteristic dependence of P_{las} on x (see Fig. 9) shows that in the case of side cooling, P_{las} at $x < x'_{B=C}$ is higher, and at $x > x'_{B=C}$ the lasing power is smaller than in its absence. The reason behind this is obviously caused by the fact that the tangential stress σ_φ increases with increasing α_3, and at $\alpha_3 > \alpha_3^{B=C}$ the disk will be damaged at smaller lasing powers (at $x < x'_{B=C}$) than at $\alpha_3 = 0$.

Therefore, side cooling plays a positive role in increasing P_{las} at any x if $\alpha_3 < \alpha_3^{B=C}$, and at $x < x'_{B=C}$, if $\alpha_3 > \alpha_3^{B=C}$. In other words, if the heat removal from the disk side face is large, tangential stresses, limiting the maximum possible lasing power, appear in the disk at large x. If the heat removal from the disk side face decreases (due to a decrease in α_3), the power P_{las} increases at any x: at $1 \leqslant x \leqslant 10$ – by many orders of magnitude and at larger x – to a lesser extent.

7. Minimal diameter of disk AE limited by the events B and C and radial distribution of the internal temperature at large lasing power

If it is needed to obtain the prescribed lasing power, expression (29) can help to estimate the minimal AE diameter providing this power at the given thickness and values of α_2 and α_3.

7.1. Detailed analysis at $P_{las} = 1$ kW

Figure 11a presents the dependence of the minimal possible AE diameter limited by the event B or C on the AE thickness when the maximal lasing power is 1 kW, the heat exchange coefficient α_2 in the case of end cooling is 1.5 W cm^{-2} K^{-1} (effective cooling) and the heat exchange coefficient α_3 on the side face varies from 0 to 1.5 W cm^{-2} K^{-1}. The maximal AE temperature not exceeding 200 °C is possible at $h < 0.237$ cm with the used parameters. One can see that in the case of the heat-insulated side face ($\alpha_3 = 0$) the required AE diameter (limited by the event B) monotonically increases with increasing the AE thickness in the range 0.01–0.3 cm. The use of side cooling with the heat exchange coefficient $\alpha_3 = 1.5$ W cm^{-2} K^{-1} allows one to decrease the diameter by 5.3 % (compared to the diameter in the case $\alpha_3 = 0$) at $h = 0.17$ cm (before the occurrence of the event C – point 0 in Fig. 11a). At $h > 0.17$ cm, the required diameter noticeably increases (the event C has a priority – dashed curve). Thus, to decrease the diameter at $h > 0.17$ cm, the heat exchange coefficient on the side face $\alpha_3 < 1.5$ W cm^{-2} K^{-1}, depending on h, is needed. This heat

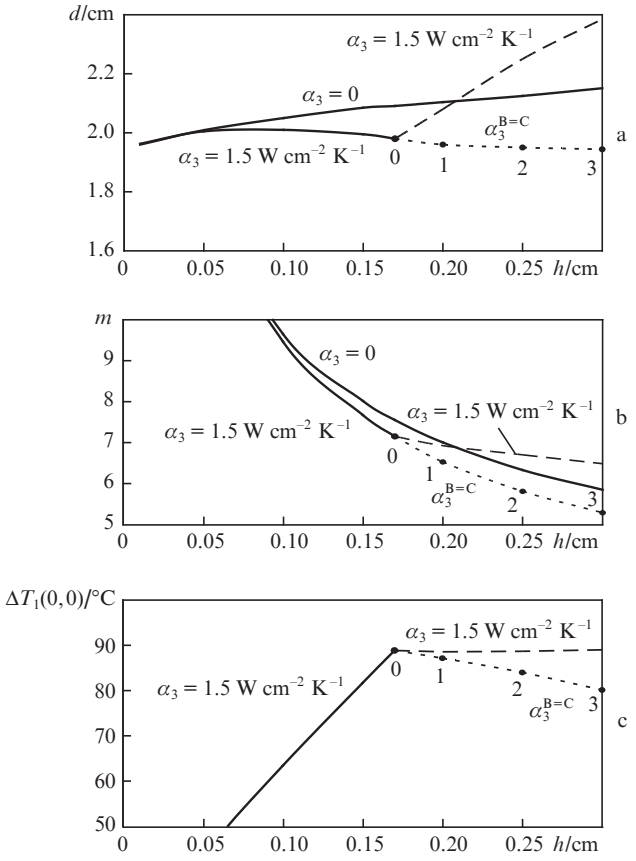

Figure 11. Minimal AE diameter (a), smoothing degree m (b), and the internal temperature drop $\Delta T_1(0,0)$ (c) for the maximal lasing power of 1 kW limited by the event B or C versus the AE thickness at α_2 = 1.5 W cm^{-2} K^{-1} and different methods of the side face cooling [α_3 = 0, 1.5 W cm^{-2} K^{-1} and $\alpha_3^{B=C}(h)$]. Solid curves are the event B, dashed curves are the event C, dotted curves are the junction of the events B and C at $\alpha_3^{B=C}$ = 1.08 (point 1), 0.71 (point 2), and 0.48 W cm^{-2} K^{-1} (point 3).

exchange coefficient is $\alpha^{B=C}(h)$ at which the AE diameter can be decreased (events B and C occur simultaneously – points 1–3).

Using the above-derived expressions for internal and external temperature drops (6)–(9) for the events B and C as well as the expression for the smoothing degree of the radial temperature profile $f(\rho,m)$ it is easy to evaluate the character of the radial temperature distribution at any point z of the AE in the case of the maximal lasing power of 1 kW (Figs 11b, c) because $\Delta T_1(\rho,z) = \Delta T_1(0,z) f(\rho,m)$. In particular, at the edges $z = 0, h$, for the event B we have

$$\Delta T_1^{B}(0,0) = \Delta T^{cr}(0,h)\frac{KM}{M+1},\ \Delta T_2^{B}(R,0) = \Delta T^{cr}(0,h)\frac{K}{M+1},$$

$$\Delta T_1^{B}(0,h) = \Delta T^{cr}(0,h)\frac{M}{M+1},\ \Delta T_2^{B}(R,h) = \Delta T^{cr}(0,h)\frac{1}{M+1},$$

and for the event C –

$$\Delta T_1^{C}(0,0) = \frac{\sigma_s}{\gamma}\frac{1}{\Theta},\ \Delta T_2^{C}(R,0) = \Delta T_1^{C}(0,0)\frac{1}{M},$$

$$\Delta T_1^{C}(0,h) = \Delta T_1^{C}(0,0)\frac{1}{K},\ \Delta T_2^{C}(R,h) = \Delta T_1^{C}(0,0)\frac{1}{KM}.$$

The end face of the disk surface (z = 0) is most strongly subjected to thermal distortions due to the face that the internal temperature drop $\Delta T_1^{B,C}(0,0)$ here is maximal; with increasing z it decreases parabolically and at point $z = h$ will be K times smaller than the maximal. Figures 11b, c show the dependence of the main parameters m and $\Delta T_1^{B,C}(0,0)$ characterising the internal temperature distribution over the radius at the maximal lasing power 1 kW on the AE thickness. At α_3 = 0 and 1.5 W cm^{-2} K^{-1} and thickness h = 0.01 cm, m is equal to 29.2, while the internal temperature drops are 0 and 21.6 °C, respectively. Using Fig. 2, we can easily estimate the internal temperature distribution profile, which has a 'shelf-like' shape. With increasing the thickness up to 0.17 cm (α_3 = 1.5 W cm^{-2} K^{-1}), the smoothing degree m decreases down to 7.15, while the internal temperature drop increases up to 88.9 °C, which forms the internal temperature distribution profile shown in Fig. 2. An increase in the thickness from 0.17 to 0.3 cm (α_3 = 1.5 W cm^{-2} K^{-1}) weakly affects the internal temperature distribution profile; in this case, the main parameters change as follows: m from 7.15 to 6.49 and $\Delta T_1^{C}(0,0)$ from 88.9 to 89 °C. The choice of the optimal $\alpha^{B=C}$ at $h > 0.17$ cm with the aim of decreasing the diameter does not lead to a gain in the smoothing of the temperature profile because a decrease in $\Delta T_1^{B=C}(0,0)$ from 88.9 °C (h = 0.17 cm) to 80.1 °C (h = 0.3 cm) is compensated for by a decrease in the smoothing degree m from 7.15 (h = 0.17 cm) to 5.29 (h = 0.3 cm).

7.2. General analysis at P_{las} = 0.1–100 kW

Figures 12–14 present the calculation results of the diameter and main parameters describing the temperature distribution over the radius, m and $\Delta T_1^{B,C}(0,0)$ for the lasing power 0.1–100 kW.

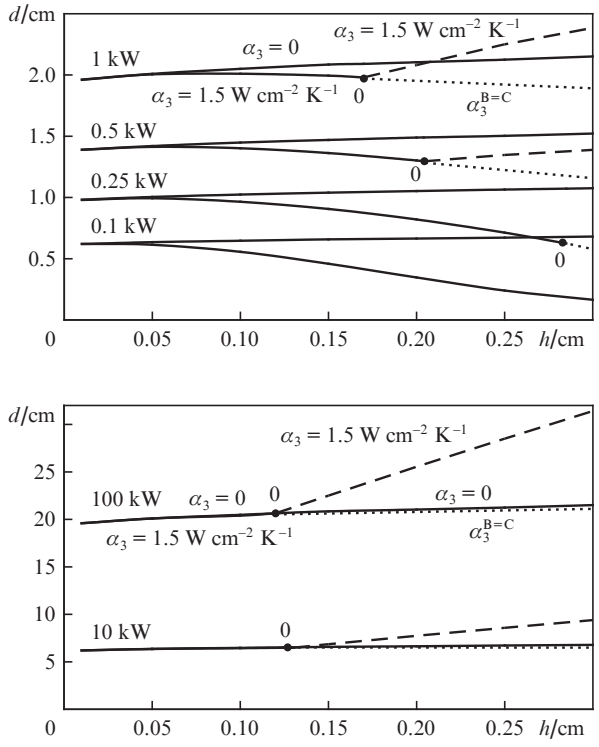

Figure 12. Minimal AE diameter for maximal lasing powers 0.1–100 kW limited by the event B or C versus the AE thickness at α_2 = 1.5 W cm^{-2} K^{-1} and different methods of the side face cooling [α_3 = 0, 1.5 W cm^{-2} K^{-1} and $\alpha_3^{B=C}(h)$]. Solid curves are the event B, dashed curves are the event C, dotted curves are the junction of the events B and C at $\alpha_3^{B=C}(h)$.

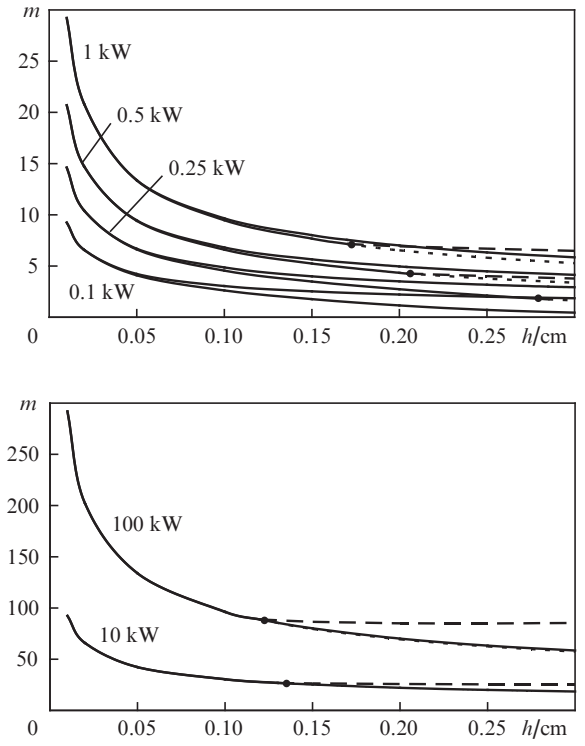

Figure 13. Smoothing degree m. Notations are the same as in Fig. 12.

For the lasing power $P_{las} = 100$ W, an increase in α_3 from 0 to 1.5 W cm^{-2} K^{-1} leads to a noticeable decrease in the diameter d; the formal calculation gives the minimal d equal to 0.026 cm at $h = 0.73$ cm (B=C) but the maximal AE temperature in this case reaches 407 °C. For $P_{las} \approx 240$ W, the minimal diameter $d = 0.55$ cm (B=C) corresponds to $h = 0.3$ cm at $\alpha_3 = 1.5$ W cm^{-2} K^{-1} and the maximal temperature 226 °C. At $P_{las} > 1$ kW, the positive effect of side cooling decreases even more (at the stage of the event B); therefore, it is preferable to exclude side cooling because in the thickness range 0.12–0.17 cm (depending on the output power), the thermal destruction has already a priority, which considerably increases the minimal diameter.

Note that the minimal diameter for the lasing power above 0.2 kW weakly depends on the thickness. To this end, we can approximately estimate it by using expression (32) at $h \to 0$ and $\alpha_3 = 0$:

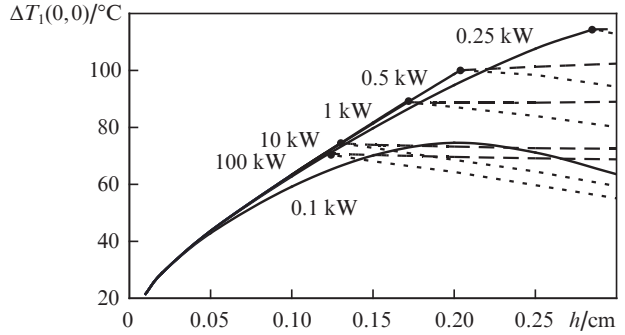

Figure 14. Internal temperature drop $\Delta T_1(0,0)$ on the axis at $z = 0$. Notations are the same as in Fig. 12.

$$d = \sqrt{\frac{4P_{las}^{B}\hbar\omega_{pump}\xi}{\pi\hbar\omega_{las}\alpha_2\Delta T^{cr}(0,h)}} = 7.44\times10^{-2}K^{-1/2}\sqrt{\frac{P_{las}^{B}}{\alpha_2}}, \quad (35)$$

where d is measured in cm, P_{las}^{B} – in W, and α_2 – in W cm^{-2} K^{-1}. Then, with the help of expression (35) we can obtain from (4) an estimating expression for the smoothing degree:

$$m = C\sqrt{\frac{2P_{las}^{B}\hbar\omega_{pump}\xi}{\pi\lambda\hbar\omega_{las}\Delta T^{cr}(0,h)h}} = 9.05\times10^{-2}\sqrt{\frac{P_{las}^{B}}{h}}, \quad (36)$$

which is independent of the heat exchange coefficient α_2.

Thus, at any lasing power, $h \leqslant 0.3$ cm and $\alpha_3 \approx 0$, as well as at $P_{las} > 0.2$ kW, $h \leqslant 0.12$ cm and $\alpha_3 \leqslant 1.5$ W cm^{-2} K^{-1}, expressions (35), (36) can help to estimate, with an accuracy no worse than $\sim 10\%$, the minimal diameter and the smoothing degree as functions of the AE thickness.

8. Conclusions

(i) We have derived an analytic expression describing with an accuracy of $\sim 10\%$ the stationary two-dimensional axially symmetric temperature distribution in a disk AE cooled from the end face and from the side face for the disk thicknesses $0.01 \leqslant h \leqslant 0.3$ cm and the diameter-to-thickness ratio $1 \leqslant x \leqslant 100$.

(ii) We have calculated the radial and tangential stresses in the disk in the case of uniform steady-state pumping. It is shown that from the point of view of thermomechanical damage the tangential stress of the disk side face constitutes the main threat.

(iii) We have estimated the limiting lasing powers, which can be obtained in a disk AE cooled from the end and side surfaces of the disk. It is shown that side cooling can decrease P_{las} in certain situations.

(iv) We have determined the priority regions in the space of the parameters k, h, x, α_2, and α_3 in which, with increasing the pump intensity, one of the three events violating the normal operation of the laser occurs first: deterioration of spectral and luminescent AE characteristics, malfunctioning of the normal cooling regime; thermomechanical disk damage.

(v) We have shown that the general smoothing of the temperature radial profile along the z axis is determined by the smoothing function $f(\rho,m)$ (characterised by the parameter m – the smoothing degree) and the temperature drop $\Delta T_1(0,z)$ (proportional to the heat exchange coefficient α_3 on the side surface). Temperature smoothing leads to smoothing of thermoelastic stresses.

(vi) If the medium cooling the side face is temperature sensitive, resulting in such undesirable effects as start of water boiling, melting of an indium substrate, etc., they should be taken into account in calculating the maximal lasing efficiency. Because in this thermal problem for the disk AE, the maximal temperature drop on the side surface is formed at $z = 0$ and $r = R$, by introducing the critical temperature drop $\Delta T_2^{cr}(R,0) = T^{cr}(R,0) - T_f$, where, for example, $T^{cr}(R,0) = 100$ °C and the coolant is water, we obtain from (5) and (8) the second critical function of heat release sources

$$q_V^{cr} = \Delta T_2^{cr}(R,0)\frac{2\alpha_3\Psi}{RK},$$

which should be also taken into account in the analysis of the events B and C. The condition $T^{cr}(R,0) = 100$ °C has the

highest effect on the maximal lasing power at the scaling parameter $x < 1$.

(vii) The limiting pump power resulting in the thermal damage due to the tangential stress at $z = 0$ and $r = R$ can be always somewhat increased, which means that the maximal lasing power can be also increased. There exist several methods to do this: not to illuminate the entire AE area, to cool additionally the disk end face (the method of a cooling jacket – export of the region in which the maximal temperature gradient is formed outside the pumped region), or to form the radial pump-power profile with a gentle slope at the side face of the AE.

References

1. Stewen C., Contag K., Larionov M., Giesen A., Hügel H. *IEEE J. Sel. Top. Quantum Electron.*, **6** (4), 650 (2000).
2. Johannsen I., Erhard S., Müller S., Stewen C., Giesen A., Contag K., in *OSA Trends in Optics and Photonics, Advanced Solid State Lasers* (Washiington, DC, Optical Society of America, 2000) Vol. 34, pp 137–143.
3. Erhard S., Karszewski M., Stewen C., Giesen A., Contag K., Voss A., in *OSA Trends in Optics and Photonics, Advanced Solid State Lasers* (Washiington, DC, Optical Society of America, 2000) Vol. 34, pp 78–84.
4. Garnov S.V., Mikhailov V.A., Serov R.V., Smirnov V.A., Tsvetkov V.B., Shcherbakov I.A. *Kvantovaya Elektron.*, **37** (10), 910 (2007) [*Quantum Electron.*, **37** (10), 910 (2007)].
5. Smirnov V.A., Shcherbakov I.A. *Kvantovaya Elektron.*, **38** (12), 1105 (2008) [*Quantum Electron.*, **38** (12), 1105 (2008)].
6. Alpat'ev A.N., Smirnov V.A., Shcherbakov I.A. *Kvantovaya Elektron.*, **39** (11), 1033 (2009) [*Quantum Electron.*, **39** (11), 1033 (2009)].
7. Kovalenko A.D. *Termouprugost'* (Thermal Elasticity) (Kiev: Izd. 'Vishcha shkola', 1975).
8. Mezenov A.V., Soms L.N., Stepanov A.I., in *Termooptika tverdotel'nykh lazerov* (Thermal Optics of Solid-State Lasers) (Leningrad: Mashinostroenie, 1986).
9. Koechner W. *Solid-State Laser Engineering* (New York: Springer, 2006).